



OPEN ACCESS

EDITED BY

Shengxian Tu,
Shanghai Jiao Tong University, China

REVIEWED BY

Zsolt Kőszegi,
University of Debrecen, Hungary
Georgios Benetos,
National and Kapodistrian University of Athens,
Greece

*CORRESPONDENCE

Anja Radunović
✉ anja.radunovic95@gmail.com

RECEIVED 11 September 2023

ACCEPTED 18 October 2023

PUBLISHED 06 November 2023

CITATION

Radunović A, Vidaković R, Timčić S,
Odanović N, Stefanović M, Lipovac M,
Krupniković K, Mandić A, Kojić D, Tomović M
and Ilić I (2023) Multislice computerized
tomography coronary angiography can be a
comparable tool to intravascular ultrasound in
evaluating “true” coronary artery bifurcations.
Front. Cardiovasc. Med. 10:1292517.
doi: 10.3389/fcvm.2023.1292517

COPYRIGHT

© 2023 Radunović, Vidaković, Timčić,
Odanović, Stefanović, Lipovac, Krupniković,
Mandić, Kojić, Tomović and Ilić. This is an open-
access article distributed under the terms of the
[Creative Commons Attribution License \(CC BY\)](https://creativecommons.org/licenses/by/4.0/).
The use, distribution or reproduction in other
forums is permitted, provided the original
author(s) and the copyright owner(s) are
credited and that the original publication in this
journal is cited, in accordance with accepted
academic practice. No use, distribution or
reproduction is permitted which does not
comply with these terms.

Multislice computerized tomography coronary angiography can be a comparable tool to intravascular ultrasound in evaluating “true” coronary artery bifurcations

Anja Radunović^{1*}, Radosav Vidaković^{2,3}, Stefan Timčić¹,
Natalija Odanović¹, Milica Stefanović², Mirko Lipovac¹,
Kosta Krupniković¹, Aleksandar Mandić¹, Dejan Kojić¹,
Milosav Tomović¹ and Ivan Ilić^{1,3}

¹Department of Cardiology, Institute for Cardiovascular Diseases Dedinje, Belgrade, Serbia, ²Department of Cardiology, Clinical Hospital Center Zemun, Belgrade, Serbia, ³Faculty of Medicine, University of Belgrade, Belgrade, Serbia

Aim: Coronary bifurcation atherosclerosis depends on its angles, flow, and extensive branching. We investigate the ability of CT coronary angiography (CTCA) to determine atherosclerotic plaque characteristics of “true” bifurcation compared with intravascular ultrasound (IVUS) and the influence on side branch (SB) fate after percutaneous coronary intervention (PCI).

Methods and results: The study included 70 patients with 72 “true” bifurcations. Most of the bifurcations were in the left anterior descending–diagonal (Dg) territory [50 out of 72 (69.4%)]. Longitudinal plaque evaluation at the polygon of confluence [carina and 5 mm proximal and distal in the main branch (MB)] showed that carina side MB and SB plaque had occurred with the lowest incidence with fibro-lipid structure (115 ± 63 HU and 89 ± 73 HU, $p < 0.001$ for all). Bland–Altman analysis showed a discrepancy in measuring mainly the lumen area between CTCA and IVUS in proximal MB [lumen 5.10, 95% CI (95% confidence interval, 4.53–5.68) mm², $p < 0.001$; vessel -1.42 , 95% CI (-2.63 to -0.21) mm², $p = 0.023$], carina MB [lumen 3.74, 95% CI (3.37–4.10) mm², $p < 0.001$; vessel -0.48 , 95% CI (-1.45 to 0.48) mm², $p = 0.322$], and distal MB [lumen 4.72, 95% CI (4.27–5.18) mm², $p < 0.001$; vessel 0.62, 95% CI (-0.53 to 1.77) mm², $p = 0.283$]. A significant correlation existed between average plaque density on CTCA with a percentage of calcified plaque on IVUS tissue characterization (proximal $r = 0.307/p = 0.024$, carina 0.469/0.008, distal 0.339/0.024, minimal lumen diameter 0.318/0.020). Circumferential plaque in the proximal MB segment remained an independent predictor of SB compromise [OR 3.962 (95% CI 1.170–13.418)].

Conclusion: Detection and characterization of atherosclerotic plaque by CTCA in non-left main “true” coronary bifurcations can provide useful information about bifurcation anatomy and plaque distribution that can predict outcomes after provisional stenting, thus guiding the interventional strategy to bifurcation PCI.

KEYWORDS

CT coronary angiography, PCI, IVUS, coronary artery bifurcation, atherosclerosis plaque

1. Introduction

Coronary artery disease (CAD) is still one of the leading causes of mortality in developed countries, and approximately 7 million people in the world every year have a confirmed diagnosis of acute coronary syndrome (ACS) (1). Percutaneous coronary interventions (PCI) in bifurcation lesions comprise approximately 15%–20% of all PCI procedures and are associated with an increased incidence of restenosis and stent thrombosis (2, 3). No single PCI technique that is universally applicable to all patients with coronary bifurcation lesions is available, but the preferred strategy for most of them, depending on distribution of atherosclerosis in main branch (MB) and side branch (SB), would be first to stent the MB across SB (4). Treatment of “true” bifurcation lesions, which have a significant stenosis of more than 50% in both MB and SB, especially if the plaque extends distally from the SB ostium, remains challenging, also often requiring stent implantation in the SB (5).

Multislice computerized tomography coronary angiography (CTCA) has become an important tool for establishing the diagnosis of ischemic heart disease, allowing detection and tissue characterization of coronary artery atherosclerotic lesions (6, 7). CTCA has been extensively explored as a non-invasive method that can provide useful information regarding plaque distribution and characteristics that can be helpful in planning and execution of complex PCI. CTCA plays a major role in PCI guidance of chronic total occlusion (CTO) that enables evaluation of occlusion length and distribution and composition of the atherosclerotic plaque (8–10). CTCA enables non-invasive evaluation of three-dimensional geometry of coronary bifurcations, including angle measurement and plaque detection. It provides complete visualization of angulation of the coronary tree preventing foreshortening and overlapping of bifurcation segments that is common in conventional angiography (11, 12). Based on the CTCA, several scoring systems were developed that served to predict the outcomes of bifurcation PCI, such as V-RESOLVE (Risk prediction of Side branch OccLusion in coronary bifurcation interVention) score (13). In comparison with intravascular ultrasound (IVUS), CTCA showed a good correlation in identification and quantification of intermediate atherosclerotic lesions (14, 15).

Therefore, we investigated whether the characteristics of atherosclerotic plaque in MB and SB in “true” non-left main bifurcation lesions, determined by CTCA, can influence the occurrence of SB compromise after MB provisional stenting and to compare bifurcation plaque analysis between CTCA and IVUS.

2. Materials and methods

The study was prospective and conducted in a PCI center of a single, high-volume tertiary university. It included patients with “true” native coronary artery bifurcations (Medina 1.0.1; 0.1.1; 1.1.1) with a visually estimated stenosis of >50% in both MB and SB, with an SB diameter greater than 2 mm. Patients were

scheduled to undergo PCI based on the history of typical stable angina, silent ischemia, and/or proven ischemia on functional testing. The study was approved by the institutional ethics committee and was completed in accordance with the Helsinki Declaration, and it was a part of the project that evaluated the use of multimodality imaging with CTCA, IVUS, and invasive coronary angiography in “true” coronary bifurcations treated with PCI according to recent guidelines (the study protocol was registered at www.clinicaltrials.gov—NCT 01943643) (4).

2.1. Study population

The study included patients with chronic coronary syndrome; therefore, patients with ACS were not included. Moreover, patients were not considered for the study if they have left ventricular ejection fraction (LVEF) of less than 30% or suffering from renal failure with estimated glomerular filtration rate (eGFR) of less than 30 ml/min/m². Patients with bifurcation lesion within the culprit artery causing myocardial infarction, grafted surgically or previously treated with PCI, were not considered for the study. Patients having medical conditions that can be a contraindication for CTCA and/or PCI were also excluded from the study. Due to planned CTCA investigation and complex PCI, we felt that it would be unethical to perform calcium scoring prior to CTCA. However, based on CTCA findings, patients with extensive calcifications at the site of bifurcation planned to be treated (with circumferential calcification greater than 180° and/or 5 mm or more in length) were excluded.

2.2. CTCA procedure

Patients underwent CTCA on Aquilion CXL 128 slice CT scanner (Toshiba Medical Systems Europe, Zoetermeer, Netherlands) using a predefined protocol and Ultravist 370 contrast agent (with an iopromide concentration of 370 mg/ml, Bayer Health Care, Germany). The angiograms were analyzed offline using dedicated software Vital Vitrea Advanced 6.2 (Vital Images, Minnetonka, MN, USA). The bifurcation lesion analysis included the measurement of proximal and distal reference vessel diameters (RVD) of the MB and RVD of the SB at the point least affected by atherosclerosis of up to 10 mm from the bifurcation's stenosis; MB vessel and lumen diameters and areas 5 mm proximal to the carina, at the carina level, and 5 mm distal to the carina (polygon of confluence); and at the site of MB's greatest luminal narrowing—minimal lumen diameter (MLD). The same analysis was performed at the SB ostium. Moreover, the angles between MB and SB were measured. The plaque analysis was performed in the longitudinal cross-section of the bifurcation at the lateral and carina sides at every previously mentioned location in the MB and SB (Figure 1). Circumferential cross-sectional plaque analysis was performed at the points of “polygon of confluence” to locate the presence of circumferential plaque. The plaques were identified at the

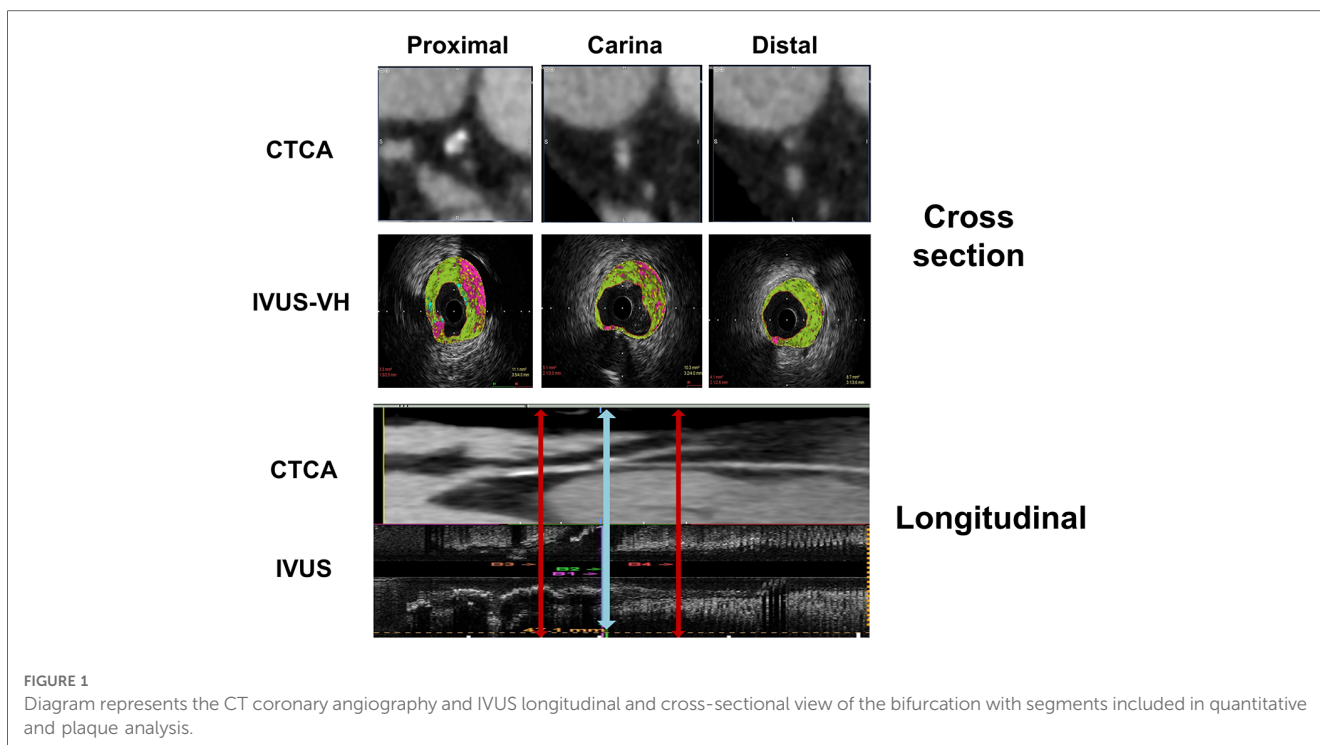


FIGURE 1
Diagram represents the CT coronary angiography and IVUS longitudinal and cross-sectional view of the bifurcation with segments included in quantitative and plaque analysis.

pericardial, myocardial, lateral, and medial sides of the vessel. Circumferential plaque was defined as the presence of atherosclerotic plaque at every side of the vessel at the predefined points in “polygon of confluence” and at the ostium of the SB (Figure 2). The plaque analysis in the longitudinal cross-section included determination of the type of the tissue based on a measured density in Hounsfield units (HU), so that the plaque with a density of up to 75 HU was marked as lipid, 76–130 HU as fibro-lipid, 131–350 HU as fibrous, and above 351 HU as calcified plaque (16).

A detailed description of CTCA procedure is available in [Supplementary Data File](#).

2.3. IVUS procedure

After placing coronary guidewires in MB and SB, MB IVUS was performed using an Opticross 40 MHz IVUS catheter (Boston Scientific Corporation/SciMed, Natick, MA, USA). The withdrawal of the catheter was performed using an automated motorized pullback at a constant speed of 0.5 mm/s. The acquired data were stored and transferred for an offline analysis using commercially available software QIvus 3.0 (Medis Medical Images Software, Leiden, Netherlands). The lumen and the media–adventitia borders were defined by automatic contour detection software with manual editing at the frames of interest.

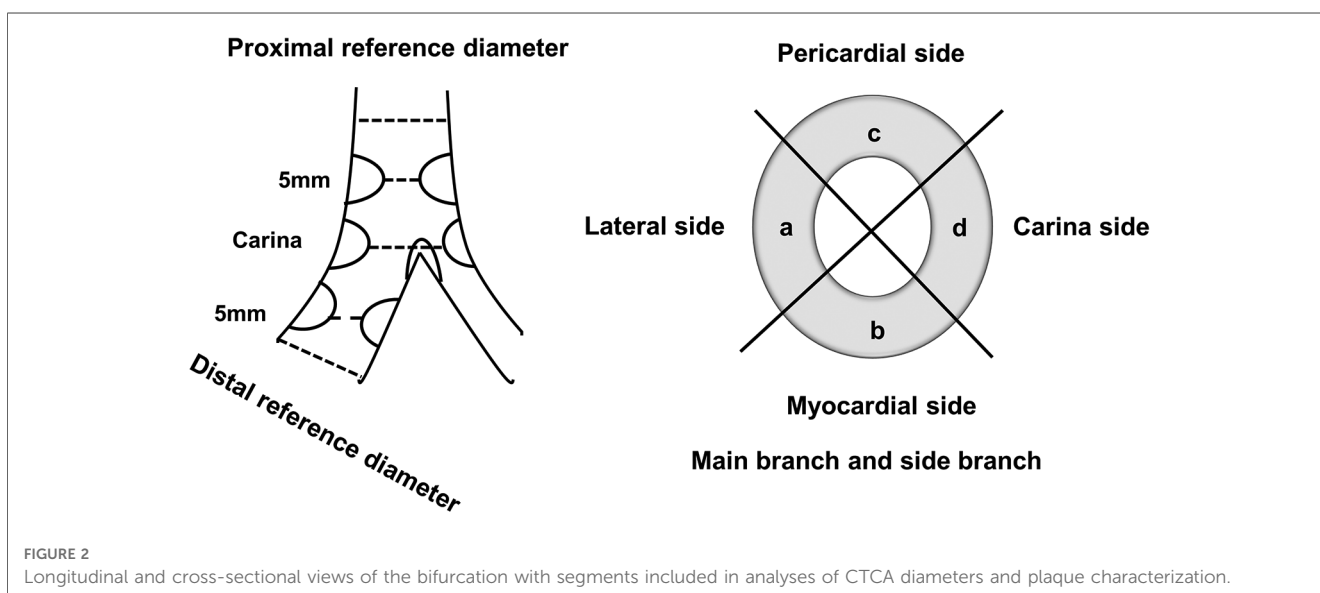


FIGURE 2
Longitudinal and cross-sectional views of the bifurcation with segments included in analyses of CTCA diameters and plaque characterization.

Tissue characterization was done using iMAP software (Boston Scientific Corporation/SciMed, Natick, MA, USA) which uses color codes to describe the composition of the atherosclerotic plaque so that the fibrous tissue is coded green, lipid as yellow, necrotic as purple, and calcified plaque as light blue. The results were expressed as the percentage of the total segmental plaque for each tissue.

The anatomical co-registration between two imaging modalities was performed by identifying the carina on IVUS longitudinal and cross-section as a last frame where the entire circumference of MB and SB can be visualized before confluence. The points 5 mm proximal and distal to the carina in “polygon of confluence” were then identified. On longitudinal IVUS recording, the distance of the MLD point from the bifurcation’s carina was calculated. The carina was identified on CTCA cross-section using the same principle as in IVUS recording, and then other three points of interest were detected using distances obtained in the IVUS longitudinal section (**Figure 1**).

2.4. PCI procedure

An initial strategy for PCI in all cases was “provisional” stenting of the MB. The choice of vascular access, guiding catheters, and coronary wires were left to the operators’ discretion. After MB predilation, a second-generation drug-eluting stent (DES) was placed across the SB, with a diameter chosen according to the visual estimate of the distal MB in accordance with Murray’s law (4). After performing the proximal optimization technique (POT) using a short non-compliant balloon catheter, coronary angiograms in two orthogonal projections were performed. If the SB coronary blood flow was less than thrombolysis in myocardial infarction (TIMI) 3, the procedure was continued with angioplasty of the SB ostium. If after angioplasty and/or kissing balloon inflation the SB TIMI flow was less than 3 and/or there was an ostial dissection, another second-generation DES was implanted in the SB using the technique chosen by the operator. A detailed description of the PCI procedure and postprocedural treatment is available in **Supplementary Data File**.

2.5. Statistical analysis

Continuous data were summarized as the means \pm SD. Categorical data were summarized as counts and percentages. Unpaired *t*-test was used for comparing the continuous variables, and the chi-squared test and Fisher’s exact test were used for categorical variables. The effect of the patient’s characteristics on the endpoint of SB compromise, defined as a decrease in flow below TIMI 3, was assessed using a logistic multivariable model, and the impact of these covariates was expressed as odds ratios with 95% confidence intervals (95% CI). A set of variables was prospectively selected, and a stepwise selection process was used to determine independent predictors of SB compromise in a multivariate analysis model. The correlation between CTCA and

IVUS was assessed using Pearson’s linear correlation. The mean differences and limits of agreement between these two imaging modalities were assessed by Bland–Altman analysis. The 95% limits of agreement were defined as the range of values within \pm 2 standard deviations (SD) from the mean difference. A *p*-value of <0.05 was considered statistically significant. All statistical analyses were performed using PASW Statistics 18.0 statistical software (SPSS Inc., Chicago, IL, USA).

3. Results

Initially 123 patients were prospectively evaluated for inclusion in the study. Eight patients denied informed consent to participate in the study, 26 patients had extensive calcifications that precluded plaque analysis, 14 patients’ angiograms did not fulfill the criteria for “true” bifurcation on CTCA due to insignificant stenosis of any of the bifurcation’s branches, and five patients had angiograms not of suitable quality for interpretation.

3.1. Clinical and PCI results

The study included 70 patients with 72 “true” non-left main bifurcations. Their mean age was 60.2 ± 9.4 years, and the 71.4% of patients were males. Patients included in the study were found to have high incidence of hypertension, dyslipidemia, previous myocardial infarction, and previous PCI (**Table 1**).

Most of the patients included in the study had two-vessel disease [one-vessel disease, 17 out of 70 (24.3%); two-vessel disease, 43 out of 70 (61.4%); and three-vessel disease, 10 out of 70 (14.3%)]. Most of the bifurcations were in the left anterior descending (LAD)—diagonal (Dg) territory. All interventions were deemed successful by the operator with final TIMI 3 flows

TABLE 1 Clinical characteristics of the patients.

Variable	<i>n</i> = 70
Age (years)	60.2 \pm 9.4
Male gender (%)	71.4
Heredity (%)	44.2
Smoking (%)	42.0
Hypertension (%)	92.7
Dyslipidemia (%)	72.4
Diabetes mellitus (%)	18.8
Insulin-dependent DM (%)	5.9
PAD (%)	5.8
Previous MI	55.1
Previous CVA (%)	2.9
Previous PCI (%)	55.0
Previous CABG (%)	0.0
BMI (kg/m ²)	28.4 \pm 3.9
LVEF (%)	51 \pm 11
eGFR (ml/min/m ²)	85.6 \pm 22.7

BMI, body mass index; CABG, coronary artery bypass grafting; CVA, cerebrovascular event; DM, diabetes mellitus; eGFR, estimated glomerular filtration rate; LVEF, left ventricular ejection fraction; PAD, peripheral arterial disease; PCI, percutaneous coronary intervention.

in MB and SB. Decreased coronary flow TIMI < 3 occurred in 17 out of 72 bifurcations (23.6%). It was treated by either balloon angioplasty only of the SB ostium [POT-side-POT, nine out of 17 (52.9%)] or stent implantation [eight out of 17 (47.1%)] followed by kissing balloon inflation and repeated POT (Table 2). During the CTCA procedure, the patients were exposed to dose-length product (DLP) of 414.18 ± 245.39 mGy cm, which was equivalent to exposure dose of 5.79 ± 3.43 mSv. The fluoroscopy time for the intervention was 48 ± 35 min, the amount of contrast used was 143 ± 57 ml, and patients' radiation exposure was 1.02 ± 0.34 Gy.

TABLE 2 Angiographic and PCI characteristics of treated bifurcations.

Bifurcation characteristics	n = 72
Location n (%)	
LAD-Dg	50 (69.4)
Cx-OM	17 (23.6)
RCA PD-PL	5 (6.9)
Medina classification n (%)	
1.0.1	16 (22.2)
0.1.1	25 (34.7)
1.1.1	31 (43.0)
RVD MB (mm)	3.6 ± 0.4
RVD SB (mm)	2.6 ± 0.5
Stent diameter in MB (mm)	3.1 ± 0.4
Stent length in MB (mm)	25.8 ± 5.8
Maximum stent inflation (atm)	14.0 ± 1.4
SB TIMI < 3 n (%)	17 (23.6)
POT-side-POT n (%)	9 (52.9)
Stent in SB n (%)	8 (47.1)

Cx, circumflex; Dg, diagonal; OM, obtuse marginal; PD, posterior descending; PL, posterolateral; POT, proximal optimization technique; RCA, right coronary artery; RVD, reference vessel diameter.

3.2. CTCA results

On CTCA, the data acquired at longitudinal cross-section of bifurcation were presented in Figure 3, including bifurcation angles with plaque densities. The average reference vessel diameters were as follows: the MB reference diameter was 3.55 ± 0.67 mm and SB ostium 2.66 ± 0.42 mm, while the MB/SB ratio was 1.3 ± 0.3. Plaques on the carina side of the bifurcation's MB and SB carina fibro-lipid were compared with the fibrous ones on the lateral side of both MB (197 ± 191 HU vs. 115 ± 63 HU, p = 0.001) and SB (132 ± 161 vs. 89 ± 73 HU, p = 0.01). In the cross-sectional view, circumferential plaque occurred most frequently at the MLD level (39 out of 72 bifurcations, 54%), while in other measured segments, its incidence was lower: proximal MB (27 out of 72, 37%), carina-level MB (26 out of 72, 36%), distal MB (21 out of 72, 29%), and SB ostium (14 out of 72, 19%). In a multivariate regression analysis that included previously recognized predictors of SB compromise (diabetes, bifurcation angle, plaque at the carina side of MB and SB, circumferential plaque proximal and at the level of carina in the MB, circumferential plaque at SB ostium, ratio of MB/SB diameters), only proximal MB circumferential atherosclerotic plaque remained an independent predictor of decreased SB flow after stent implantation [3.962 (95% CI 1.170–13.418), p = 0.027] (Table 3).

3.3. Quantitative results of CTCA and IVUS

The differences in vessel and lumen area measurements between CTCA and IVUS of the MB were pronounced regarding the lumen area at the MB carina and distal segment, together with the MLD segment. On the other hand, the significant

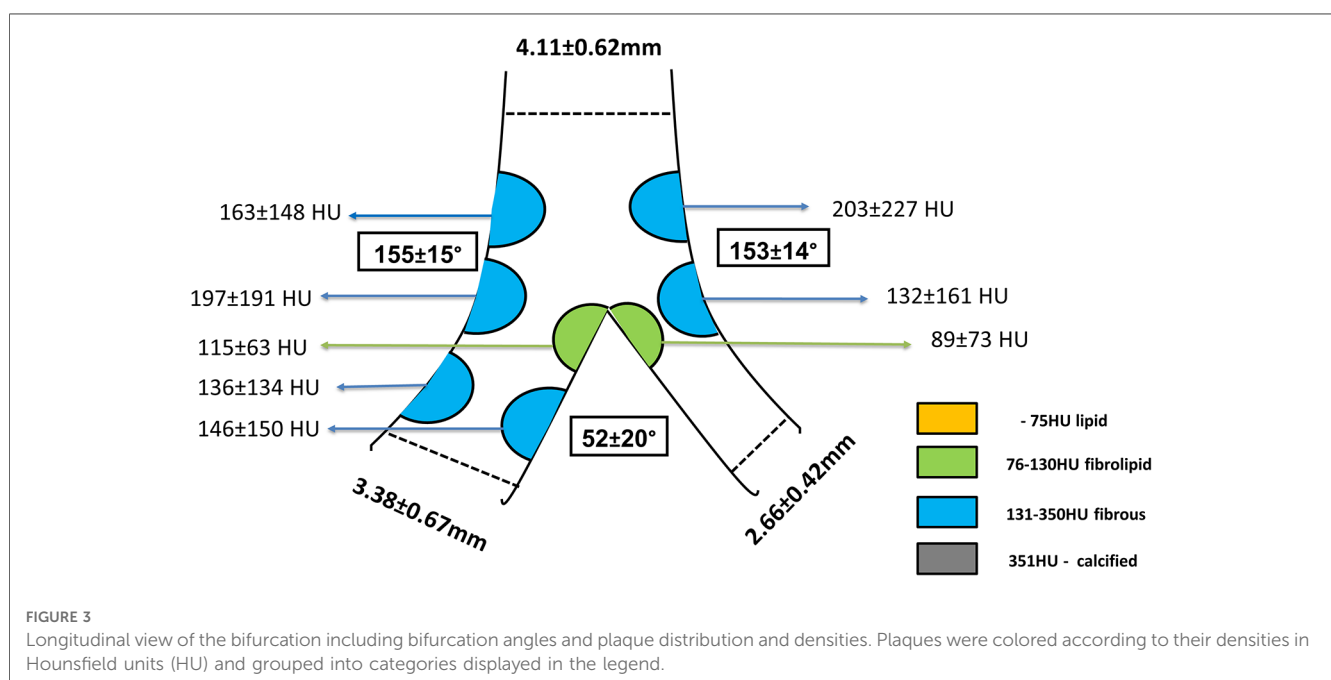


TABLE 3 Univariate and multivariate predictors of SB compromise (TIMI < 3).

	Univariate		Multivariate	
	OR (95% CI)	p-value	OR (95% CI)	p-Value
Presence of diabetes	1.333 (0.355–5.011)	0.670	—	—
Bifurcation angle	1.041 (0.995–1.090)	0.085	1.041 (0.995–1.090)	0.084
MB/SB reference diameters	0.794 (0.082–7.711)	0.842	—	—
SB carina plaque in longitudinal view	1.307 (0.413–4.133)	0.649	—	—
MB carina plaque in longitudinal view	0.891 (0.289–2.748)	0.840	—	—
Circumferential plaque at MB carina	1.450 (0.477–4.409)	0.513	—	—
Circumferential plaque at proximal MB	3.480 (1.114–10.864)	0.032	3.962 (1.170–13.418)	0.027
Circumferential plaque at SB ostium	3.250 (0.883–11.967)	0.076	1.432 (0.450–4.561)	0.543

TABLE 4 Mean values and differences in the lumen and vessel area of the bifurcation's MB measured using CTCA and IVUS.

Variable	CTCA	IVUS	Difference	p-Value
Proximal segment				
Lumen area (mm ²)	4.80 ± 3.19	5.41 ± 2.41	−0.61 ± 3.63	0.214
Vessel area (mm ²)	13.70 ± 4.25	12.28 ± 3.11	1.42 ± 4.53	0.023
Carina segment				
Lumen area (mm ²)	2.95 ± 1.63	4.53 ± 1.79	−1.58 ± 2.07	<0.001
Vessel area (mm ²)	10.49 ± 4.11	10.01 ± 2.97	0.48 ± 3.62	0.322
Distal segment				
Lumen area (mm ²)	3.87 ± 2.06	5.59 ± 2.34	−1.72 ± 2.81	<0.001
Vessel area (mm ²)	9.62 ± 3.85	10.24 ± 3.59	−0.62 ± 4.29	0.283
MLD segment				
Lumen area (mm ²)	0.97 ± 0.49	3.19 ± 0.82	−2.22 ± 0.95	<0.001
Vessel area (mm ²)	13.78 ± 5.00	10.75 ± 2.84	3.03 ± 4.89	<0.001

differences in the vessel area were shown on proximal MB and MLD segments of bifurcation (Table 4). Bland–Altman analysis showed a discrepancy in measuring mainly the lumen area between CTCA and IVUS in proximal MB [lumen 5.10, 95% CI (4.53–5.68) mm², $p < 0.001$; vessel −1.42, 95% CI (−2.63 to −0.21) mm², $p = 0.023$], carina MB [lumen 3.74, 95% CI (3.37–4.10) mm², $p < 0.001$; vessel −0.48, 95% CI (−1.45 to 0.48) mm², $p = 0.322$], and distal MB [lumen 4.72, 95% CI (4.27–5.18) mm², $p < 0.001$; vessel 0.62, 95% CI (−0.53 to 1.77) mm², $p = 0.283$]. The plot demonstrated that most of the measurements were within the limits of 2 SD (Figure 4A–C).

When comparing tissue characteristics of the MB as assessed by CTCA and IVUS, most of the plaques were classified as fibrotic on CTCA which is in concordance with fibrous tissue dominance on IVUS virtual histology (VH) (Table 5). A significant correlation was noted between MB average plaque density in HU on CTCA with the percentage of calcified atherosclerotic plaque on IVUS tissue characterization at every level of “polygon of confluence” (Figure 5).

4. Discussion

We conducted the study in which we evaluated the use of CTCA in a complex, bifurcation lesion that had advanced atherosclerotic disease with significant plaques in both MB and

SB. Our study demonstrated that in “true” non-left main bifurcations plaques located on the carina side of MB and SB have lower densities compared with plaques located on the lateral walls of the MB and SB on CTCA. Importantly, atherosclerotic plaques that “encroach” the entire circumference of the proximal segment of the MB were independently associated with SB flow compromise after “provisional” stenting of the MB and POT. Fair correlation existed between CTCA and IVUS in measuring vessel diameters and when comparing plaque density on CTCA and percentage of calcified plaque on IVUS VH.

Atherosclerotic plaques in coronary artery bifurcations tend to develop in the areas of low endothelial shear stress (ESS), at the lateral walls of bifurcations, where the endothelium is stimulated by local growth factors and relatively slow, laminar blood flow. On the other hand, in the areas with high ESS located usually at the flow divider of the bifurcation, plaque rarely develops and has different characteristics (17, 18). In a study of 65 bifurcations, van der Giessen et al. demonstrated that atherosclerotic plaques mostly developed in the areas of low wall shear stress and that calcium-rich plaques are situated in the lateral portions (19). It was also demonstrated by Eshthardi et al. that areas with high ESS show a negative correlation with specific plaque characteristics (necrotic core and dense calcium) (20).

Our series of bifurcations comply with an observed pattern, and plaques at the carina side of MB and SB were less frequently found compared with plaques at the lateral side. We found that plaques at the lateral side of the bifurcation contain more dense plaques compared with the plaques on the flow divider side.

The SB compromise, defined as a decrease in coronary flow below TIMI 3, occurred in almost one-fifth of our patients. The presence of the plaque on the carina side in the SB was associated with SB compromise in univariate analysis, but this relationship was not confirmed in multivariable model. In our study, only circumferential plaque in the proximal segment of the MB was independently associated with SB compromise. This could be the consequence of the large plaque volume in the proximal MB being pushed toward the SB ostium by stent implantation which, when added to ostial stenosis of the SB, might result in a critical stenosis or occlusion of the SB and decreased TIMI flow (snow plough effect). This finding corroborates with large registry of bifurcation PCI which demonstrated that significant stenosis of proximal MB is associated with SB compromise (21, 22). Moreover, an optical

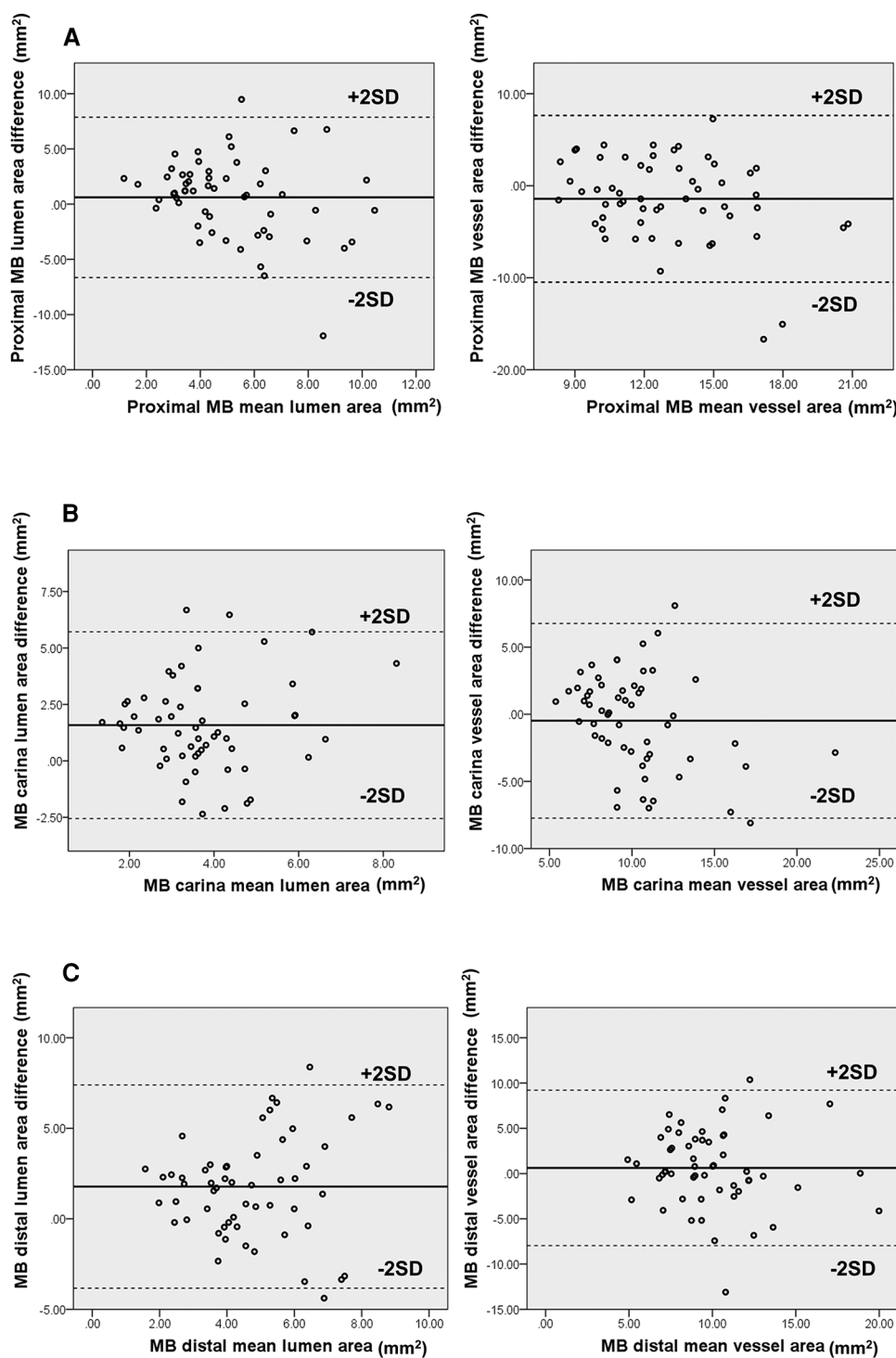


FIGURE 4 (A–C) Diagram displays Bland–Altman plots of lumen and vessel area measurements’ differences in mm² using CTCA versus IVUS at proximal (A), carina (B), and distal segment (C) of MB bifurcation. The diagram shows moderate correlation with wide limits of agreement.

coherence tomography study by Kini et al. demonstrated that patients with SB occlusion had greater diameter stenosis of proximal MB, although MB stenosis was not an independent predictor of SB compromise, as opposed to the lipid content of the proximal MB plaque (23). Recently developed prediction scores that use CT often depict low attenuation and calcified

plaque of proximal MB as significant contributors to SB compromise (24, 25). The diameter ratio between MB and SB on CTCA did not show relevant association with SB compromise in our study, contrary to the validated RESOLVE score that include the MB/SB ratio as an important predictor of SB decreased TIMI flow. The reason for this may be attributed to the complexity of

TABLE 5 Bifurcation’s tissue characterization assessed by CTCA and IVUS.

Variable	Proximal segment	Carina segment	Distal segment	MLD segment
CTCA				
Average plaque density (HU)	183 ± 188	156 ± 127	138 ± 142	160 ± 202
Plaque classification ^a	F	F	F	F
IVUS				
Fibrous plaque (%)	66 ± 13	61 ± 13	61 ± 14	53 ± 13
Lipid plaque (%)	10 ± 4	11 ± 4	12 ± 4	11 ± 4
Necrotic plaque (%)	22 ± 11	25 ± 11	25 ± 11	32 ± 11
Calcified plaque (%)	2 ± 2	3 ± 3	2 ± 3	4 ± 2

^aPlaque classification based on density lipid (L) (–30–75 HU), fibro-lipid (FL) (76–130 HU), fibrous (F) (131–350 HU), and calcified (C) (more than 351 HU).

bifurcations included in our study leading to very high RESOLVE scores in which the MB/SB ratio would have relatively small contribution especially if we know that the average MB/SB ratio in our study was 1.3 ± 0.3 . This value would only add two points to the RESOLVE score which, in our group of patients, would be more affected by diameter stenoses of MB and SB, bifurcation angle, and plaque distribution (13, 26).

Our study included patients with large, advanced plaque burden of the bifurcation, in whom we were unable to perform volumetric plaque analysis to evaluate the possible effect of “plaque shift” on the SB fate. This limitation of our study in evaluating plaque behavior attributed to MB stent implantation must be noted. A precise automated volumetric plaque analysis on CTCA would add valuable information about plaque burden and its behavior after stent implantation.

Previous studies demonstrated a good correlation between CTCA and IVUS in quantifying intermediate coronary atherosclerotic lesions with the notion that CTCA overestimates the lumen area (26, 27).

In our study measurements of the vessel area were similar at all levels of bifurcation, which was not true for lumen measurement, especially at the MLD point in the MB. In concert with previous studies, in our population CTCA overestimated the lumen area of the bifurcation. The average plaque density at the MLD level was 144 ± 138 HU with a maximum density of 541 HU. The calcium density on CTCA approaches the density of contrast fluid and could impede detection of lumen and vessel borders leading to the evidence that inaccurate CTCA vessel and plaque quantitative measurements are associated with greater calcified plaque volume, increased percentage of calcified plaque, and lumen diameter smaller than 2.8 mm (28–30). It should be noted that we did not perform calcium scoring according to Agatston score in order to reduce radiation exposure, and we excluded patients with type III and IV calcified lesions on CT. These lesions could interfere with the vessel analysis on CT and influence the correlation between measurements performed on CTCA and IVUS (31). Since our trial included vessels with relatively large diameters (Table 2), the accuracy of CTCA has been preserved, because it has been previously shown that small vessels and extensive calcification interfere with the accuracy of CT evaluation (32).

We found a moderate correlation for average plaque density on CTCA and percentage of calcified plaque on IVUS tissue characterization in all segments of the bifurcation’s MB. The reason for this could be sought in the observation that IVUS VH software often misclassifies the zone of acoustic shadow behind the calcified plaque and that spatial resolution of the CT scanner that we used may not be able to reliably discern fibrous and lipid plaque, as IVUS can do (33, 34). If we combine shortcomings of CT coronary angiography regarding differentiation of fibrous and lipidic plaques and the effects of calcified plaque on IVUS VH that can be the reason for relatively moderate correlation regarding between these modalities regarding plaque

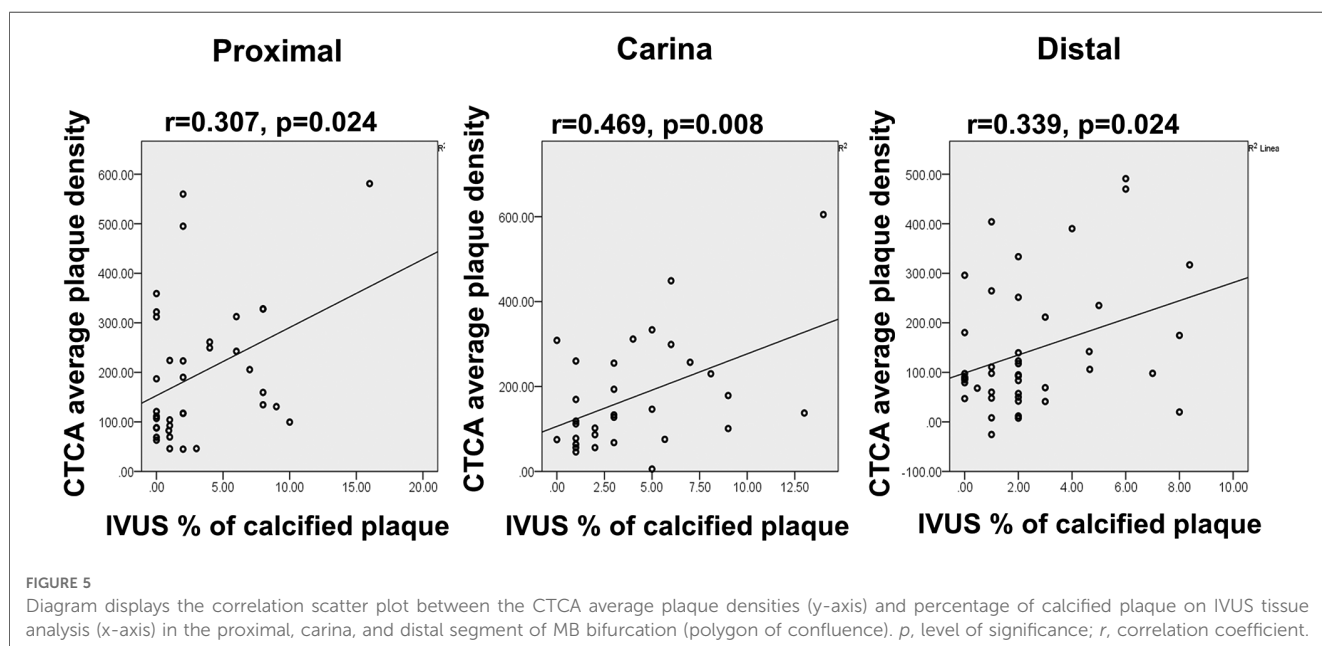


FIGURE 5 Diagram displays the correlation scatter plot between the CTCA average plaque densities (y-axis) and percentage of calcified plaque on IVUS tissue analysis (x-axis) in the proximal, carina, and distal segment of MB bifurcation (polygon of confluence). *p*, level of significance; *r*, correlation coefficient.

identification. The IVUS VH software itself, due to these issues, has been abandoned in the new versions of IVUS proprietary software.

4.1. Limitations of the study

It should be noted that we performed semiautomated anatomical co-registration between CTCA and IVUS which can lead to a certain bias in measurements and interpretation of the results. Automated software that can perform precise co-registration would lead to increased accuracy of the measurements and better correlation between imaging modalities (35). When evaluating circumference cross-section of the MB and SB, we were not able to perform plaque thickness quantitative analysis that could have influence on carina shift and potential SB compromise.

4.2. Impact on daily practice

Thorough plaque identification and quantification using CTCA could give a better insight for an interventionalist about the distribution and extent of atherosclerotic disease in complex coronary bifurcation. This non-invasively acquired information can cause a treating physician to anticipate difficulties in PCI and to decide to change the initial strategy toward a more complex one and to make a better choice of stent diameter and length. All this can improve the use of resources and minimize procedural risks.

5. Conclusion

Detection and characterization of atherosclerotic plaque by CT coronary angiography in non-left main “true” coronary bifurcations can provide useful information about bifurcation anatomy and plaque distribution that can predict outcomes after provisional stenting, thus guiding the interventional strategy to bifurcation PCI. It also gives comparable results to IVUS regarding vessel sizing and plaque characterization.

Data availability statement

The original contributions presented in the study are included in the article/**Supplementary Material**, further inquiries can be directed to the corresponding author.

Ethics statement

The studies involving humans were approved by Ethics Committee of the Clinical Hospital Center Zemun. The studies

were conducted in accordance with the local legislation and institutional requirements. The participants provided their written informed consent to participate in this study.

Author contributions

AR: Conceptualization, Investigation, Visualization, Writing – original draft, Writing – review & editing. RV: Project administration, Writing – original draft. ST: Methodology, Writing – review & editing. NO: Data curation, Writing – original draft. MS: Resources, Writing – review & editing. ML: Software, Writing – original draft. KK: Formal Analysis, Writing – review & editing. AM: Investigation, Writing – original draft. DK: Supervision, Validation, Writing – review & editing. MT: Supervision, Validation, Writing – original draft. II: Conceptualization, Formal Analysis, Funding acquisition, Investigation, Project administration, Software, Supervision, Validation, Writing – original draft, Writing – review & editing.

Funding

The authors declare that no financial support was received for the research, authorship, and/or publication of this article.

Conflict of interest

The authors declare that the research was conducted in the absence of any commercial or financial relationships that could be construed as a potential conflict of interest.

Publisher's note

All claims expressed in this article are solely those of the authors and do not necessarily represent those of their affiliated organizations, or those of the publisher, the editors and the reviewers. Any product that may be evaluated in this article, or claim that may be made by its manufacturer, is not guaranteed or endorsed by the publisher.

Supplementary material

The Supplementary Material for this article can be found online at: <https://www.frontiersin.org/articles/10.3389/fcvm.2023.1292517/full#supplementary-material>

References

- Bhatt DL, Lopes RD, Harrington RA. Diagnosis and treatment of acute coronary syndromes: a review. *JAMA*. (2022) 327:662–75; Erratum in *JAMA*. (2022) 327:1710. doi: 10.1001/jama.2022.0358.
- Colombo A, Moses JW, Morice MC, Ludwig J, Holmes DR Jr, Spanos V, et al. Randomized study to evaluate sirolimus-eluting stents implanted at coronary bifurcation lesions. *Circulation*. (2004) 109:1244–9. doi: 10.1161/01.CIR.0000118474.71662.E3
- Routledge HC, Lefèvre T, Colombo A, Oldroyd KG, Hamm CW, Guagliumi G, et al. Three-year clinical outcome of percutaneous treatment of bifurcation lesions in multivessel coronary artery disease with the sirolimus-eluting stent: insights from the arterial revascularisation therapies study, part II (ARTS II). *EuroIntervention*. (2009) 5:190–6. doi: 10.4244/EIJV5I2A30
- Burzotta F, Lassen JF, Lefèvre T, Banning AP, Chatzizisis YS, Johnson TW, et al. Percutaneous coronary intervention for bifurcation coronary lesions: the 15th consensus document from the European bifurcation club. *EuroIntervention*. (2021) 16(16):1307–17. doi: 10.4244/EIJ-D-20-00169
- Lassen JF, Albiero R, Johnson TW, Burzotta F, Lefèvre T, Iles TL, et al. Treatment of coronary bifurcation lesions, part II: implanting two stents. The 16th expert consensus document of the European Bifurcation Club. *EuroIntervention*. (2022) 18(6):457–70. doi: 10.4244/EIJ-D-22-00166
- Cademartiri F, Casolo G, Clemente A, Seitun S, Mantini C, Bossone E, et al. Coronary CT angiography: a guide to examination, interpretation, and clinical indications. *Expert Rev Cardiovasc Ther*. (2021) 19(5):413–25. doi: 10.1080/14779072.2021.1915132
- Peper J, Becker LM, van den Berg H, Bor WL, Brouwer J, Nijenhuis VJ, et al. Diagnostic performance of CCTA and CT-FFR for the detection of CAD in TAVR work-up. *JACC Cardiovasc Interv*. (2022) 15(11):1140–9. doi: 10.1016/j.jcin.2022.03.025
- Werner GS, Hecht H, Stone GW. Utility of CT angiography to guide coronary intervention of CTO. *JACC Cardiovasc Imaging*. (2015) 8:814–6. doi: 10.1016/j.jcmg.2015.04.009
- Opolski MP, Achenbach S. CT angiography for revascularization of CTO: crossing the borders of diagnosis and treatment. *JACC Cardiovasc Imaging*. (2015) 8:846–58. doi: 10.1016/j.jcmg.2015.05.001
- Luo C, Huang M, Li J, Liang C, Zhang Q, Liu H, et al. Predictors of interventional success of antegrade PCI for CTO. *JACC Cardiovasc Imaging*. (2015) 8:804–13. doi: 10.1016/j.jcmg.2015.04.008
- Tu S, Jing J, Holm NR, Onsea K, Zhang T, Adriaenssens T, et al. In vivo assessment of bifurcation optimal viewing angles and bifurcation angles by three-dimensional (3D) quantitative coronary angiography. *Int J Cardiovasc Imaging*. (2012) 28:1617–25. doi: 10.1007/s10554-011-9996-x
- Huo Y, Finet G, Lefevre T, Louvard Y, Moussa I, Kassab GS. Which diameter and angle rule provides optimal flow patterns in a coronary bifurcation? *J Biomech*. (2012) 45:1273–9. doi: 10.1016/j.jbiomech.2012.01.033
- Opolski MP, Grodecki K, Staruch AD, Michalowska AM, Kepka C, Wolny R, et al. Accuracy of RESOLVE score derived from coronary computed tomography versus visual angiography to predict side branch occlusion in percutaneous bifurcation intervention. *J Cardiovasc Comput Tomogr*. (2020) 14(3):258–65. doi: 10.1016/j.jcct.2019.11.007
- Leber AW, Becker A, Knez A, von Ziegler F, Sirol M, Nikolaou K, et al. Accuracy of 64-slice computed tomography to classify and quantify plaque volumes in the proximal coronary system: a comparative study using intravascular ultrasound. *J Am Coll Cardiol*. (2006) 47:672–7. doi: 10.1016/j.jacc.2005.10.058
- Papadopoulos SL, Neeffjes LA, Schaap M, Li HL, Capuano E, van der Giessen AG, et al. Detection and quantification of coronary atherosclerotic plaque by 64-slice multidetector CT: a systematic head-to-head comparison with intravascular ultrasound. *Atherosclerosis*. (2011) 219:163–70. doi: 10.1016/j.atherosclerosis.2011.07.005
- Varga-Szemes A, Maurovich-Horvat P, Schoepf UJ, Zsarnoczay E, Pelberg R, Stone GW, et al. Computed tomography assessment of coronary atherosclerosis: from threshold-based evaluation to histologically validated plaque quantification. *J Thorac Imaging*. (2023) 38(4):226–34. doi: 10.1097/RTI.0000000000000711
- Grottum P, Svindland A, Walloe L. Localization of atherosclerotic lesions in the bifurcation of the main left coronary artery. *Atherosclerosis*. (1983) 47:55–62. doi: 10.1016/0021-9150(83)90071-0
- Stone PH, Saito S, Takahashi S, Makita Y, Nakamura S, Kawasaki T, et al. Prediction of progression of coronary artery disease and clinical outcomes using vascular profiling of endothelial shear stress and arterial plaque characteristics: the PREDICTION study. *Circulation*. (2012) 126:172–81. doi: 10.1161/CIRCULATIONAHA.112.096438
- Van der Giessen AG, Wentzel JJ, Meijboom WB, Mollet NR, van der Steen AF, van de Vosse FN, et al. Plaque and shear stress distribution in human coronary bifurcations: a multislice computed tomography study. *Eurointervention*. (2009) 4:654–61. doi: 10.4244/EIJV4I5A109
- Eshetehardi P, McDaniel MC, Suo J, Dhawan SS, Timmins LH, Binongo JN, et al. Association of coronary wall shear stress with atherosclerotic plaque burden, composition, and distribution in patients with coronary artery disease. *J Am Heart Assoc*. (2012) 1:e002543. doi: 10.1161/JAHA.112.002543
- Hahn JY, Chun WJ, Kim JH, Song YB, Oh JH, Koo BK, et al. Predictors and outcomes of side branch occlusion after main vessel stenting in coronary bifurcation lesions: results from the COBIS II registry (COronary BIfurcation Stenting). *J Am Coll Cardiol*. (2013) 62:1654–9. doi: 10.1016/j.jacc.2013.07.041
- Park JJ, Chun EJ, Cho YS, Oh IY, Yoon CH, Suh JW, et al. Potential predictors of side-branch occlusion in bifurcation lesions after percutaneous coronary intervention: a coronary CT angiography study. *Radiology*. (2014) 271:711–20. doi: 10.1148/radiol.14131959
- Kini AS, Yoshimura T, Vengrenyuk Y, Amirian J, Hasan C, Baber U, et al. Plaque morphology predictors of side branch occlusion after main vessel stenting in coronary bifurcation lesions: optical coherence tomography imaging study. *JACC Cardiovasc Interv*. (2016) 9:862–5. doi: 10.1016/j.jcin.2016.02.022
- Grodecki K, Cadet S, Staruch AD, Michalowska AM, Kepka C, Wolny R, et al. Noncalcified plaque burden quantified from coronary computed tomography angiography improves prediction of side branch occlusion after main vessel stenting in bifurcation lesions: results from the CT-PRECISION registry. *Clin Res Cardiol*. (2021) 110(1):114–23. doi: 10.1007/s00392-020-01658-1
- Lee SH, Lee JM, Song YB, Park TK, Yang JH, Hahn JY, et al. Prediction of side branch occlusions in percutaneous coronary interventions by coronary computed tomography: the CT bifurcation score as a novel tool for predicting intraprocedural side branch occlusion. *EuroIntervention*. (2019) 15(9):e788–95. doi: 10.4244/EIJ-D-18-00113
- Dou K, Zhang D, Xu B, Yang Y, Yin D, Qiao S, et al. An angiographic tool for risk prediction of side branch occlusion in coronary bifurcation intervention: the RESOLVE score system (risk prEdiction of Side branch Occlusion in coronary bifurcation interVention). *JACC Cardiovasc Interv*. (2015) 8(1 Pt A):39–46. doi: 10.1016/j.jcin.2014.08.011
- De Graaf MA, Broersen A, Kitslaar PH, Roos CJ, Dijkstra J, Lelieveldt BP, et al. Automatic quantification and characterization of coronary atherosclerosis with computed tomography coronary angiography: cross-correlation with intravascular ultrasound virtual histology. *Int J Cardiovasc Imaging*. (2013) 29(5):1177–90. doi: 10.1007/s10554-013-0194-x
- Voros S, Rinehart S, Qian Z, Joshi P, Vazquez G, Fischer C, et al. Coronary atherosclerosis imaging by coronary CT angiography: current status, correlation with intravascular interrogation and meta-analysis. *JACC Cardiovasc Imaging*. (2011) 4(5):537–48. doi: 10.1016/j.jcmg.2011.03.006
- Noll D, Kruk M, Demkow M, Pręgowski J, Kaczmarek E, Kryczka K, et al. Patterns of coronary calcification and their impact on the diagnostic accuracy of computed tomography coronary angiography. *J Comput Assist Tomogr*. (2018) 42(2):263–8. doi: 10.1097/RCT.0000000000000681
- Kruk M, Noll D, Achenbach S, Mintz GS, Pręgowski J, Kaczmarek E, et al. Impact of coronary artery calcium characteristics on accuracy of CT angiography. *JACC Cardiovasc Imaging*. (2014) 7(1):49–58. doi: 10.1016/j.jcmg.2013.07.013
- Qi L, Tang L-J, Xu Y, Zhu X-M, Zhang Y-D, Shi H-B, et al. The diagnostic performance of coronary CT angiography for the assessment of coronary stenosis in calcified plaque. *PLoS One*. (2016) 11(5):e0154852. doi: 10.1371/journal.pone.0154852
- Cao JJ, Shen L, Nguyen J, Rapelje K, Porter C, Shlofmitz E, et al. Accuracy and limitation of plaque detection by coronary CTA: a section-to-section comparison with optical coherence tomography. *Sci Rep*. (2023) 13(1):11845. doi: 10.1038/s41598-023-38675-9
- Nakanishi R, Motoyama S, Leipsic J, Budoff MJ. How accurate is atherosclerosis imaging by coronary computed tomography angiography? *J Cardiovasc Comput Tomogr*. (2019) 13(5):254–60. doi: 10.1016/j.jcct.2019.06.005
- Truesdell AG, Alasnag MA, Kaul P, Rab ST, Riley RF, Young MN, et al. Intravascular imaging during percutaneous coronary intervention: JACC state-of-the-art review. *J Am Coll Cardiol*. (2023) 81(6):590–605. doi: 10.1016/j.jacc.2022.11.045
- Collet C, Onuma Y, Grundeken MJ, Miyazaki Y, Bittercourt M, Kitslaar P, et al. In vitro validation of coronary CT angiography for the evaluation of complex lesions. *EuroIntervention*. (2018) 13(15):e1823–30. doi: 10.4244/EIJ-D-17-00326